Available online at www.sciencedirect.com
ScienceDirect
Advances in Space Research 58 (2016) 1793–1806
ADVANCES IN SPACE RESEARCH (a COSPAR publication)
www.elsevier.com/locate/asr

Potential applications of skip SMV with thrust engine

Weilin Wang [a,b,*], Al Savvaris [b]

[a] National University of Defense Technology, Hunan, China
[b] Cranfield University, Bedford, UK

Received 14 March 2016; received in revised form 11 June 2016; accepted 21 June 2016
Available online 25 June 2016

Abstract

This paper investigates the potential applications of Space Maneuver Vehicles (SMV) with skip trajectory. Due to soaring space operations over the past decades, the risk of space debris has considerably increased such as collision risks with space asset, human property on ground and even aviation. Many active debris removal methods have been investigated and in this paper, a debris remediation method is first proposed based on skip SMV. The key point is to perform controlled re-entry. These vehicles are expected to achieve a trans-atmospheric maneuver with thrust engine. If debris is released at altitude below 80 km, debris could be captured by the atmosphere drag force and re-entry interface prediction accuracy is improved. Moreover if the debris is released in a cargo at a much lower altitude, this technique protects high value space asset from break up by the atmosphere and improves landing accuracy. To demonstrate the feasibility of this concept, the present paper presents the simulation results for two specific mission profiles: (1) descent to predetermined altitude; (2) descent to predetermined point (altitude, longitude and latitude).

The evolutionary collocation method is adopted for skip trajectory optimization due to its global optimality and high-accuracy. This method is actually a two-step optimization approach based on the heuristic algorithm and the collocation method. The optimal-control problem is transformed into a nonlinear programming problem (NLP) which can be efficiently and accurately solved by the sequential quadratic programming (SQP) procedure. However, such a method is sensitive to initial values. To reduce the sensitivity problem, genetic algorithm (GA) is adopted to refine the grids and provide near optimum initial values. By comparing the simulation data from different scenarios, it is found that skip SMV is feasible in active debris removal and the evolutionary collocation method gives a truthful re-entry trajectory that satisfies the path and boundary constraints.

Keywords: Space Maneuver Vehicles; Active debris removal; Controlled re-entry; Evolutionary collocation; Skip trajectory optimization

1. Introduction

There are more than 20,000 tracked objects in space. Among them, only 1000 are functioning satellite and others are space debris. Those debris mainly come from uncontrolled spacecraft, lost equipment, rocket stages, fragments from disintegration or collisions, causing great risks to unmanned- and manned-spacecraft in the space and human activities on Earth (Liou, 2011).

Although break up of debris from the altitude of 80 km, part of total mass will survive re-entry and impact on Earth surface, thus probably poses dangers to human and property on the ground. Almost 70% of re-entry objects are uncontrolled and the debris spread over long ground track. To protect the near-Earth space and reduce the threat by implementing controlled re-entry, the most significant issue at the moment is to develop a reliable scientific method for remediation of space debris, particularly in LEO, which is known as active debris removal (ADR).

* Corresponding author at: National University of Defense Technology, Hunan, China.
E-mail address: wangweilin@nudt.edu.cn (W. Wang).

http://dx.doi.org/10.1016/j.asr.2016.06.028
0273-1177/

Many missions have been proposed or under development for active debris removal such as Clean Space One of Switzerland aiming to drag the debris to re-entry, Service Orientated ADR (SOADR) by ESA, Orbital Transfer Vehicle of CNES which is designed to remove large debris, and Deutsche Orbital Servicing Mission of DLR which is designed to rendezvous with a non-cooperative and tumbling spacecraft (Bonnal et al., 2013).

2. Potential applications of SMV with skip trajectory

With enhanced development of spacecraft capability, there is an expansion of Space Maneuver Vehicles (SMV): unscrewed, reusable payload carriers with significant maneuvering capabilities for a dynamic mission profile (AFRL, 2004). Skip re-entry is one special trans-atmospheric maneuver. Skip re-entry is widely addressed in return mission of deep space exploration vehicles for the purpose of vehicles deceleration. However the flight is unpowered and the vehicle is a glider. In the present paper, a new concept is proposed that SMV has thrust capability. This kind of SMV could descend to lower altitude and then go back to LEO with thrust engine. Although there is no relevant study about skip SMV, we here proposed this concept and demonstrated its potential applications in the following sections.

2.1. Potential application in active debris removal

The SMV could be used to support many missions, e.g. technology validation; space surveillance; on-orbit servicing; satellite deployment or retrieval; orbital debris mitigation and remediation. Among those applications, debris removal missions are the most promising including orbit changing (transfer debris or malfunctioning satellite to disposal regions in which the debris will not interfere with future space operations) and using atmosphere drag force to capture debris through controlled re-entry, etc. ADR concentrates on existing large orbital debris objects in LEO such as large booster, upper stages and defunct satellites lacking capability of controlled re-entry, which can prevent catastrophic evolutionary growth of debris. According to the classification of debris, skip SMV in ADR aims at addressing two problems: (1) reducing risks of useless space debris to ground. SMV improves re-entry interface accuracy by release debris at a pre-determined attitude and lower altitude leads to higher impact point prediction accuracy; (2) retrieving high value space property by a heat shielding cargo. Improved landing accuracy reduces difficulty for search and rescue. Those two goals are carefully discussed in the Sections 2.1.1 and 2.1.2.

2.1.1. Ability to reduce debris risk to ground

Improving the prediction accuracy of re-entry interface is critical to decrease casualty expectation caused by ground impact or breakup of hazardous debris (Kai et al., 2015).

The debris could be captured by net, robotic arm, or other clamping mechanisms, and then released at predetermined altitude in order to improve the prediction accuracy of re-entry interface. As air density is quite low at altitudes above 80 km, the more time debris spend in the atmosphere, the less accuracy the landing point can obtain due to uncertainty in debris attitude, atmosphere model, gas–surface interactions model and drag coefficient, etc. Kai et al. (2015) gives a general calculation of accumulated error. The result shows that $\pm$(10–25)% error in time of re-entry leads to $\pm$4050 km uncertainty in re-entry point. To make things worse, it is impossible to predict impact point of surviving fragments. It is practicable for landing on Pacific Ocean, but for more precise landing on ground with small area, it is infeasible.

In addition, space systems in LEO re-enter atmosphere at very shallow angle. At very shallow angle of re-entry, the behavior of space objects is similar to a pebble skipping across the surface of a pond when approaching the upper layers of the atmosphere. So it is necessary to go deep into atmosphere for larger braking force. To increase accuracy, space tug could be used for fast and steep re-entry, but it is impossible for reusability. The skip capability of SMV provides an alternative solution for controlled debris re-entry.

2.1.2. Ability to retrieve high value object

For retrieval of disabled satellite with remaining high value, it is a better choice to re-entry within a heat shielding cargo to avoid breakup due to higher density atmosphere. SMV releases the cargo at a lower altitude and then parachute works to slow down the cargo further. Compared with the landing case of retrieving satellites, it will consume less fuel and be able to implement multi missions because new launch of SMV from sea level will cost more energy compared with skip trajectory by which the vehicle goes back to orbit with high initial velocity. For retrieval of high value object, it is necessary to increase landing prediction accuracy. Otherwise, if the landing prediction area is too big, it will be difficult for on-ground rescuers to locate the cargo, which may fail the retrieval mission.

To improve landing accuracy and narrow ground footprint, it is preferable to release debris at lower altitude and even at predetermined point. The mission profile can be divided into four stages: (1) phasing and rendezvous; (2) debris capture; (3) skip re-entry and release the debris; (4) SMV goes back to orbit preparing for next mission.

2.2. Some other potential applications

In addition to application in ADR, Skip SMV also shows great potential for other operations. For example, the skip SMV could be used in Mars landing missions to release lander and then go back to orbit around Mars waiting for return to Earth. The skip trajectory could be used to dissipate heat and slow down the vehicle with more hopping. In addition, landing accuracy can be improved by releasing the lander at specific altitude (position) with appropriate velocity and prolonged travel range. Further, the skip SMV could also be implemented in over flight of ground target for surveillance purpose, etc.

2.3. Feasibility analysis

This concept is totally new and has a high requirement for the vehicle design and fuel, however it could survive in orbit for longer time and save fuel because it is possible for SMV to implement several skip missions once launched into orbit. Furthermore, such operation in space is expensive but affordable for retrieving satellites.

It will be viable in near future and many preliminary practical experiment and studies are already or being conducted. Advanced Re-entry Vehicle (ARV) is an evolution of ATV which is designed to return conditioned payloads and equipment to Earth after retirement of space shuttle (Bottacini et al., 2011). Orbital Test Vehicle is a reusable unmanned spacecraft and able to re-enter Earth's atmosphere for multi times. Actually, it is a mini space shuttle and the forth flight test is under conduction (Grantz, 2011). The Dream Chaser derived from HL-20 lifting body is a reusable crewed space plane which can operate in suborbital or orbital orbit. Its primary mission is to resupply ISS and download from space station (Howard et al., 2011). Bettinger and Black (2014) introduced a new concept TAVs which is designed to complete orbital change maneuver and overfly specified ground target. Virgili et al. (2015) studied a novel method to control re-entry location using aerodynamic drag which shows potential application in increasing precision of debris re-entry point. Moshman and Proulx (2014) studied the reachable area of hypersonic vehicle with thrust engine which concludes that the presence of an engine is most advantageous for potential maneuver or retargeting.

In Section 3, the concept of skip re-entry with thrust will be defined in detail. In Sections 4 and 5, based on the evolutionary collocation method, simulation is conducted to demonstrate the feasibility of proposed concept. And different scenarios are discussed to illustrate the problem better. Section 6 summarizes the whole work of this paper.

3. Problem definition

One of the many issues encountered in the development of skip SMV is to establish the dynamic and control equations of the vehicle with thrust capability during its re-entry into the Earth's atmosphere and to optimize its trajectory accordingly. Several methods (Duan and Li, 2015; Zhao et al., 2014; Zondervan, 1984) have been proposed to optimize the trajectory of a spacecraft entering the atmosphere however most of them relate the optimization to a landing scenario, aiming at improving the control over the range and the touchdown accuracy.

The proposed investigation in this paper will focus on the atmospheric skip of SMV, targeting the entry into the atmosphere down to a predetermined altitude or point (including altitude, longitude and latitude) and the required controls involved in returning to orbit. Du et al. (2014) studied the skip re-entry of deep-space spacecraft with high speed over first cosmic velocity, however a high thrust engine would be necessary for SMV to return to low orbit in this paper.

To find an analytic solution to the general trajectory optimization problem is difficult, instead, many numerical methods have been proposed to solve a particular profile. The main difficulty of a trans-atmospheric entry is the rapid change of atmosphere, whereas the current gradient method used for trajectory optimization is time- and memory-consuming due to the large gradients which forces the algorithm to refine the grids and leads to a significant increase in computation time.

In order to circumvent the limitation brought by the classic gradient techniques, this paper will work on direct trajectory optimization method rather than indirect methods. The solution proposed in this paper is to implement a higher non-gradient optimizer to guide the collocation grids and help smooth the control over the state discontinuities. Collocation method is applied to transform the trajectory optimization problem into a nonlinear programming problem (NLP). Then sequential quadratic programming (SQP) method is used to solve constrained nonlinear programming problem, and thus named as evolutionary collocation method. Wang et al. (2015) has preliminarily studied the difference between two heuristic optimization methods, GA and PSO. In this paper, GA is adopted due to its higher accuracy of global optimization.

General skip re-entry problem can be divided into 5 phases: initial roll, down control, up control, Kepler and final entry. Phase 5 (landing) has been thoroughly studied. Considering the mission of SMV is to arrive at a predetermined position with specific altitude, the most challenging phases 2 and 3 will be highlighted in this paper (see Fig. 1).

In this section we present the re-entry optimization problem including the atmospheric model, nonlinear dynamics, the constraints and the cost function.

3.1. Atmospheric model

For improved accuracy on the guidance before the initial entry and after the exit, the atmosphere model is built up to 1000 km from the ESDU 77021 documentation (RAS, 2005).

3.2. Dynamic model

Our initial implementation uses the physical characteristics of the NASA space shuttle found in the literature (Zondervan, 1984). The original scenario was set up in British units so most of the literature followed the trend. For this work, international standard units were used except heating flux. Interface between optimization routines and high-level modeling packages is well established with MATLAB, however models and methods can be easily

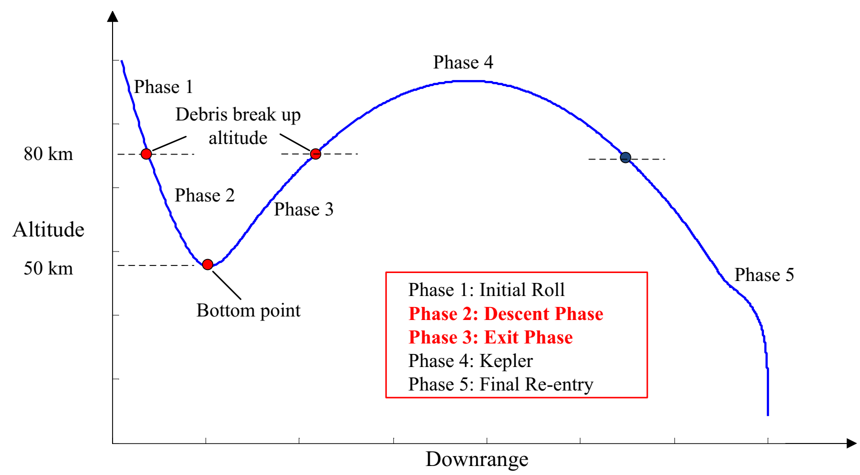

Fig. 1. Whole phase description of skip re-entry.

modified. The motion equations of the space shuttle with thrust capability are established with a minor correction of Moshman and Proulx (2014):

$$\dot{r} = v \sin\gamma \tag{1}$$

$$\dot{\phi} = \frac{v\cos\gamma\cos\psi}{r\cos\theta} \tag{2}$$

$$\dot{\theta} = \frac{v\cos\gamma\sin\psi}{r} \tag{3}$$

$$\dot{v} = \frac{T\cos\alpha - D}{m} - g\sin\gamma \tag{4}$$

$$\dot{\gamma} = \frac{L\cos\sigma + T\sin\alpha\cos\sigma}{mv} - \frac{g\cos\gamma}{v} + \frac{v\cos\gamma}{r} \tag{5}$$

$$\dot{\psi} = \frac{L\sin\sigma + T\sin\alpha\sin\sigma}{mv\cos\gamma} + \frac{v\cos\gamma\sin\psi\tan\phi}{r} \tag{6}$$

$$\dot{m} = -\frac{T}{I_{sp}g} \tag{7}$$

$$\dot{\alpha} = K_\alpha(\alpha_C - \alpha),\ \dot{\sigma} = K_\sigma(\sigma_C - \sigma),\ \dot{T} = K_T(T_C - T) \tag{8}$$

where r, ϕ, θ, v, γ, ψ, m, α, σ, T are state variables, representing radial position, latitude, longitude, velocity, flight path angle, heading angle, mass, angle of attack, bank angle and thrust respectively. Here, angle of attack (α_C), bank angle (σ_C) and thrust (T_C) denote control signals. First-order control system is applied in which K_α, K_σ, K_T are constant control gains and the control rates are limited in this manner. The lag between control signals and actual state variables is used to imitate actuator dynamics. K_α, K_σ, K_T are set as 0.001, 0.001, 0.005, respectively. L and D are the lift acceleration and drag acceleration respectively, which can be defined as:

$$L = \rho V^2 S C_L/(2m) \tag{9}$$

$$D = \rho V^2 S C_D/(2m) \tag{10}$$

where C_L is the lift coefficient, C_D is the drag coefficient and S is reference surface area. ρ is the density which can be achieved by ESDU 77021 toolbox. The aerodynamic parameters can refer to Zondervan (1984).

3.3. Solutions for optimization

The collocation method discretizes all state and control variables. Then the SMV skip trajectory optimization problem is transformed into a nonlinear programming problem containing equality and inequality constraints on the boundary conditions and path (Betts, 2010).

$$\min J = f(x) \tag{11}$$

$$h_i(x) = 0,\ i = 1, 2, \ldots, p \tag{12}$$

$$g_j(x) \geqslant 0,\ j = p+1, \ldots, q \tag{13}$$

a. Genetic algorithm

GA is one kind of evolution algorithms, which generates solutions to optimization problems using techniques inspired by natural evolution, e.g. inheritance, mutation, selection and crossover. It is regarded as one of the most robust and reliable optimization algorithms and has no requirement for gradient information or initial guess. GA is widely used on some large-scale nonlinear global optimization problems (Betts, 1998).

b. Collocation method

Equal step collocation method is applied in Wang et al. (2015). Several well-known pseudo-spectral methods have been developed for solving optimal control problems such as the Legendre pseudo-spectral method, Radau pseudo-spectral method and the Gauss pseudo-spectral method. Radau and Gauss methods outperform the Legendre method in accuracy with comparable computational efficiency. However, the Legendre method based on Gauss–Lobatto points (LGL) is the most appropriate method for solving infinite-horizon optimal control problems with

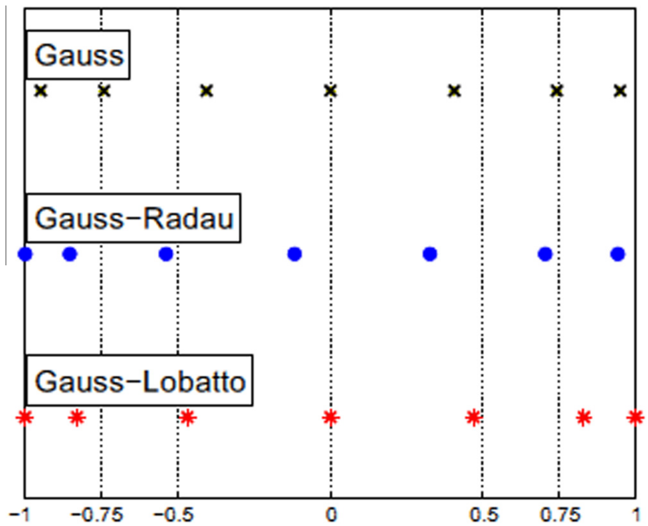

Fig. 2. Nodes distribution of three collocation methods.

arbitrary boundary conditions in skip re-entry, especially when the boundary constraints are functions of initial conditions or final conditions, Gauss and Radau pseudo-spectral methods may not converge (Fahroo and Ross, 2008). In this paper the LGL method is applied (see Fig. 2).

There are more collocation points at the boundary point, so it is preferable to divide whole phase into two separate phases at the bottom point. Then the number of collocation points around the bottom point will be larger, and the accuracy would be higher around bottom point.

c. Sequential quadratic programming

The SQP algorithm proposed by Powell is known as an efficient iterative method for NLP problems (Gill and Wong, 2012). The optimization result of GA guides the collocation grids, and then the SQP is applied to search local optimum close to the initial value to achieve an optimum of the NLP problem.

d. Optimization classification

In this paper, two types of optimization strategies are studied according to mission requirement. The difference is the initial value provided by GA. For descent to predetermined point, constraints are so higher that it is difficult for GA to converge, so it is better to divide whole phase into two parts and provide an initial value to SQP as illustrated in Fig. 3. However, for descent to a predetermined altitude without other constraints, it is appropriate to take the descent and exit as a whole phase. So in Fig. 3, step 1 and step 2 will be integrated as one step.

Fig. 3 gives a chronological view of the method: (1) Trajectory optimization for the descent. (2) Trajectory optimization for the exit. (3) Join the 2 paths on a new mesh

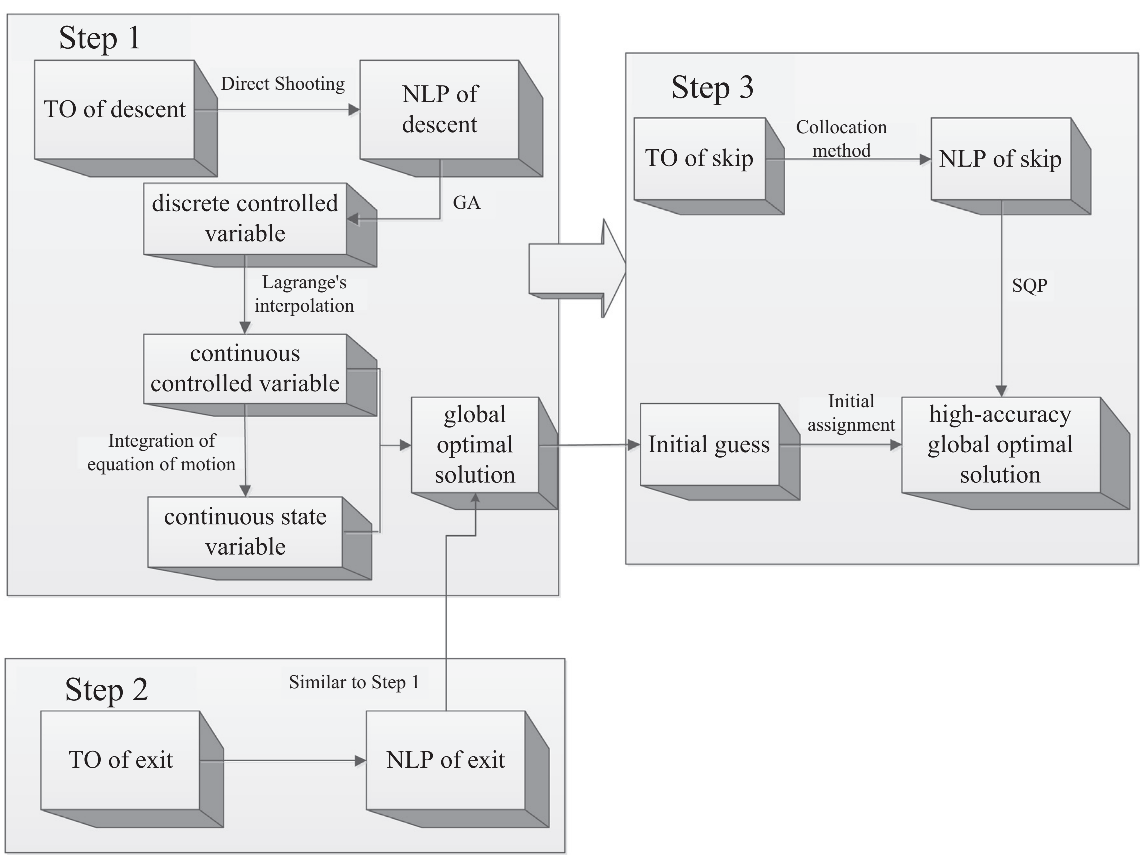

Fig. 3. Flow chart of trajectory optimization (TO).

with collocation method. Then the optimal solution of NLP is obtained using SQP on the complete trajectory.

3.4. Optimization objective and constraints

3.4.1. Optimization objective

Three single objectives may be considered including: (1) To minimize time, J_t; (2) To minimize fuel consumption, J_f; (3) To minimize total heating, J_h. For multi objective optimization, the weighting method is adopted with corresponding weighting coefficients.

$$J = \omega_t J_t + \omega_f J_f + \omega_h J_h \tag{14}$$

where $\omega_i = \frac{\omega_i'}{J_{imax}}$, and $\sum \omega_i' = 1,\ i = t,\ f,\ h.$ J_{imax} is used for order-of-magnitude agreement denoting the maximum possible value of J_i.

3.4.2. Path constraints

(1) Heating flux constraint

As the velocity of vehicle is less than 7.5 km/s, convective mode of heat transfer is the dominant form. The maximum heating rate usually happens at the bottom altitude which is closely related to velocity, height and angle of attack.

$$\dot{Q} = 17700\left(c_0 + c_1\alpha + c_2\alpha^2 + c_3\alpha^3\right)\sqrt{\rho}\left(10^{-4}v\right)^{3.07} \tag{15}$$

where $c_0,\ c_1,\ c_2,\ c_3$ are coefficients with fixed values (Zondervan, 1984). ρ is atmospheric density.

(2) Load and dynamic pressure

$$n_L = \frac{\sqrt{L^2 + D^2}}{mg_0} \tag{16}$$

$$q = \frac{1}{2}\rho v^2 \tag{17}$$

3.4.3. Boundary constraints

(1) Position constraints

Altitude constraints on descent to predetermined altitude are: $h_b \to 50$ km, $h_f \to 80$ km, which represent the altitude at bottom point and final state, respectively.

For descent to pre-determined point, there are more constraints on position apart from altitude. It is assumed that a special point is chosen with latitude and longitude both equaling to zero, i.e. $\phi \to 0,\ \theta \to 0$.

(2) Time constraint

To guarantee the complement of the SMV process, the time is limited as shown in Table 1.

Table 1
Simulation parameter setting.

Boundary conditions	Initial state	Final state
Height (km)	80	80
Velocity (km/s)	7.5	Free
Flight path angle (rad)	−0.0174	Free
Mass (kg)	90,719	Free
Longitude (rad)	−0.785	Free
Latitude (rad)	−0.174	Free
Heading angle (rad)	0	Free
AOA (rad)	0.698	Free
Bank angle (rad)	0.698	Free
Optimization constraints		
Number of collocation nodes	60	
Thrust (N)	$<2 * 10^6$	
Heat flux (BTU/ft^2/s, MW/m^2)	<200/2.2	
Dynamic pressure (N/m^2)	<13,000	
Load (/g_0)	<2.5	
Angle of attack (rad)	$\left[-\frac{\pi}{2};\frac{\pi}{2}\right]$	
Bank angle (rad)	$\left[-\frac{\pi}{2};\frac{\pi}{2}\right]$	
Time (s)	[500; 5000]	

3.4.4. Control constraints

(1) Constraints on angle of attack (AoA) and bank angle

Initial values are assumed to be the same for different scenarios and simple constraints are adopted which are shown in Table 1.

(2) Thrust constraint

To lift off, space shuttle has two solid rocket boosters each providing a thrust of 12,500 kN and three main engines each providing a thrust of 2170 kN, so the total thrust is about 30,000 kN. The main engine is able to operate for 7.5 h before requiring major maintenance.

In this paper, the maximum thrust is assumed to be 2000 kN which equals the thrust of one main engine. In Section 4, effect of thrust capability on optimization is discussed with different limitations on maximum thrust.

It should be noted that in Zondervan (1984), the maximum heating flux $\dot{Q}_{max} = 70\ \mathrm{BTU/ft^2/s}$, but it is an orginal value of NASA space shuttle nearly forty years ago. Considering the new mission requirement of rapid change in dynamics at the bottom altitude, a relatively high value is applied here.

Table 2 gives the state at bottom point. The requirement for latitude and longitude is only used in the mission of descent to predetermined point in Section 5.

Table 2
State at bottom point.

State of bottom point	Value
Height (km)	50
Velocity (km/s)	>3
Flight path angle (rad)	>0
Latitude (rad)	0
Longitude (rad)	0

- Other constraints

Longitude and latitude error for descent to point: [−0.01, 0.01] rad.

Altitude error: [−200, 200] m.

4. Simulation result of descent to predetermined altitude

In this part, the simulation of descent to predetermined altitude is conducted. There is no constraint on the longitude and latitude of bottom point.

4.1. Single objective optimization-to minimize fuel consumption

For SMV which implements skip mission, the fuel consumption is the most important factor which should be considered as the optimization objective.

4.1.1. Comparison between different altitudes

Fig. 4 shows the result for three different altitudes: 50 km, 60 km and 70 km. If the vehicle goes lower, velocity at bottom point is further reduced. Moreover, there are more hops for lower altitude and fuel consumption is greater than other two cases.

From Fig. 5 we can see that peak of path constraints occurs near the bottom point which is different from the skip reentry for landing. The values of three constraints are larger for descent to lower altitude because of denser atmosphere. Comparison between Figs. 4 and 5 shows that the crest of hop in altitude typically corresponds to a trough of hop in path constraints.

For the case of descent to 50 km, the constraint of dynamic pressure is active, which means the dynamic pressure is the dominant constraint for optimization. This can be deduced from Eq. (17) as atmosphere density is much larger than the other two cases although velocity is a little smaller.

Different altitudes indicate different landing accuracy and pose various requirements for SMV such as the thrust capability and path constraints. If altitude is lower, the prediction of landing location would be more precise because debris would spend less time in atmosphere before landing. Ground footprint would be narrower, consequently it will reduce the hazard to ground and improve the landing accuracy for retrieval of satellites corresponding to two potential applications of SMV in Section 2.1. However, it is difficult to define a minimal altitude of SMV, and the most appropriate altitude should be determined by a compromise between landing accuracy requirement, available fuel and path constraints.

4.1.2. Comparison between different thrust

From Fig. 4 we can see that, the peak of thrust for descent to 50 km reaches about 50 percent of maximum thrust. In order to show the effect of thrust on skip re-entry, three cases with much smaller thrust capabilities are discussed. Three thrust capabilities are: (a) 10 percent of maximum thrust; (b) 5 percent of maximum thrust; (c) 2.5 percent of maximum thrust, and the maximum thrust is 2000 kN.

From the subfigure of altitude we can see that if the constraint value on thrust is smaller, skip mission takes longer time and there will be more hops. Besides, the thrust has to work during descent phase because the thrust is not enough to lift vehicle up to exit atmosphere. Subfigure of bank angle shows that the bank angle descends gradually to small value to provide larger lift force in the last two cases.

Generally, small thrust can save fuel by comparing Figs. 4 and 6. However, if the thrust is too small, actuator has to work for longer time and fuel consumption is a little larger. From the subfigure of mass we can also see that, the minimum fuel consumption occupies just 6 percent of total mass which is a small value. It means that it is possible for

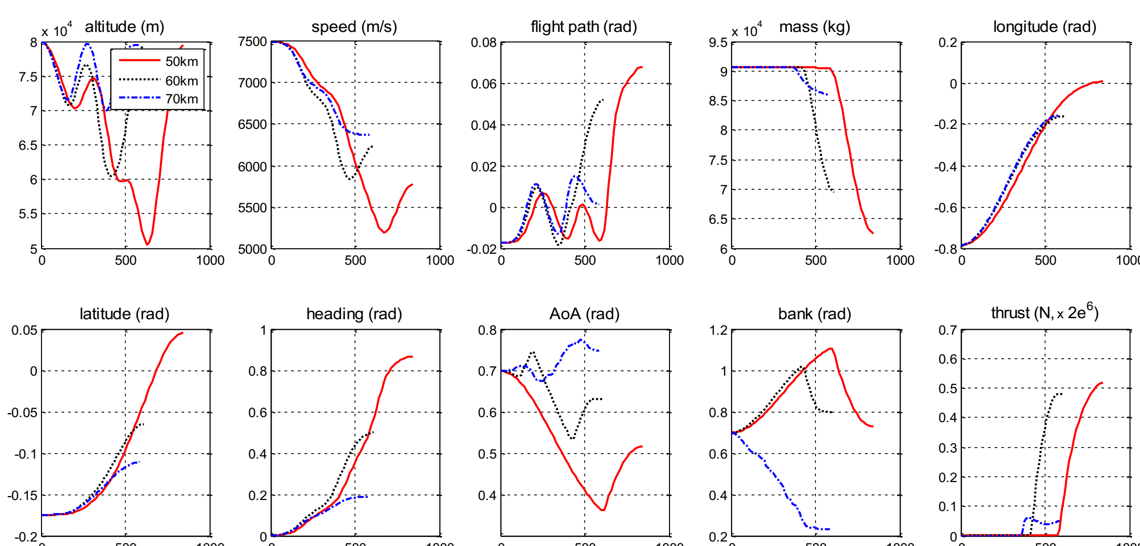

Fig. 4. State curves for SMV re-entry.

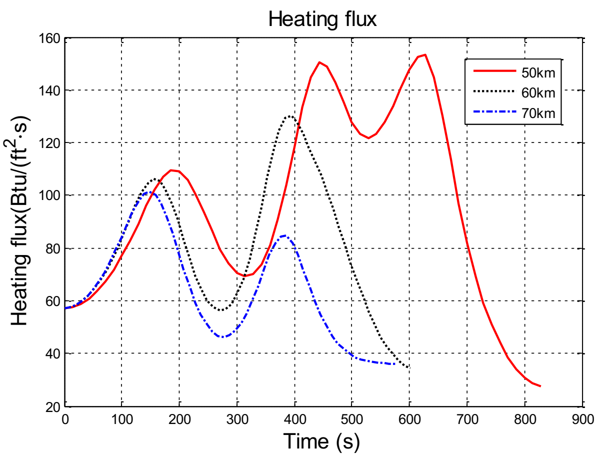

(a) Heating flux time history

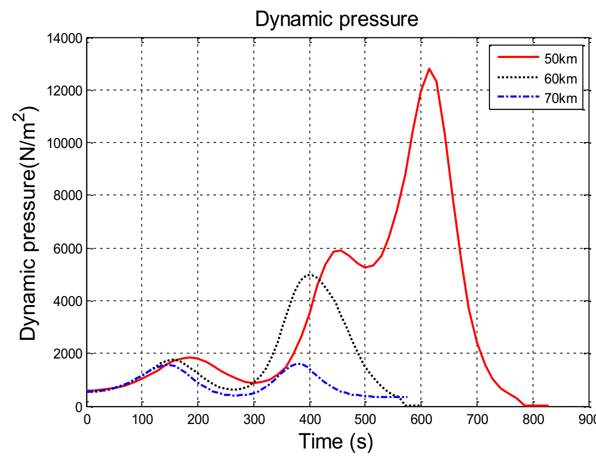

(b) Dynamic pressure time history

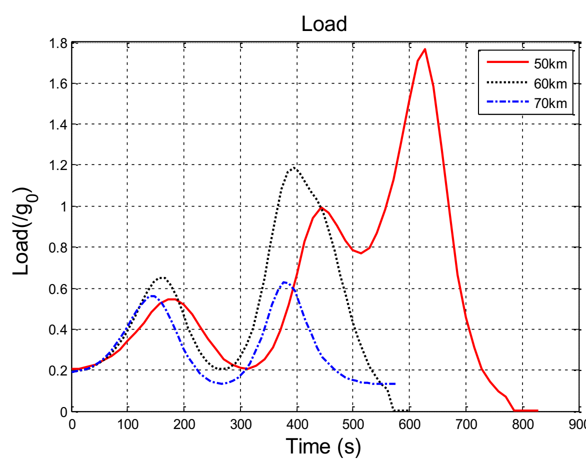

(c) Load time history

Fig. 5. Curves of path constraint.

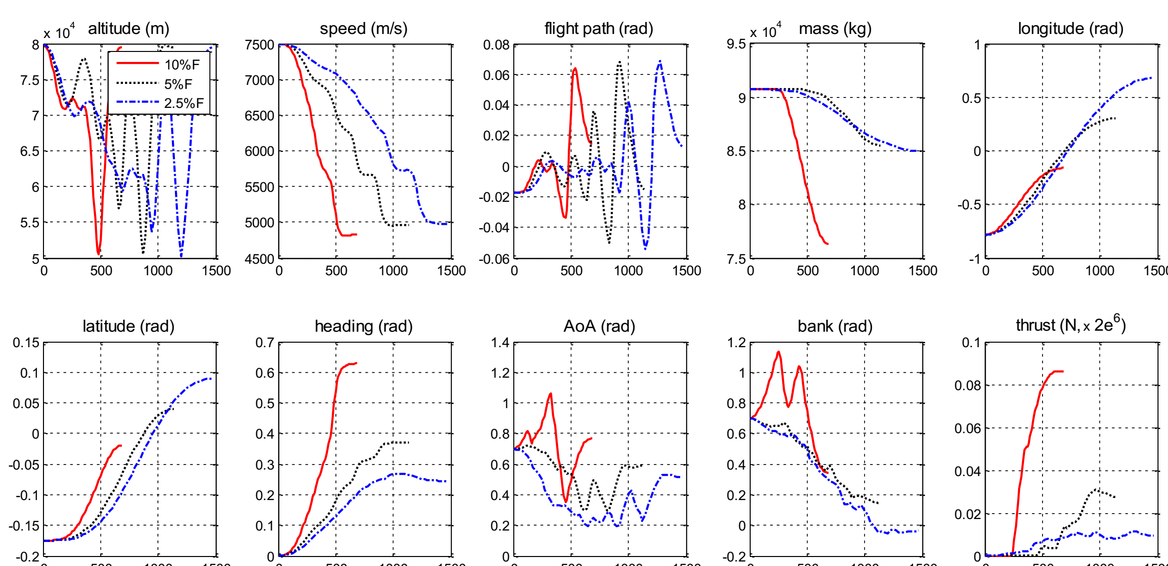

Fig. 6. State curves for SMV re-entry (10%F indicates 10% of maximum thrust).

SMV to implement several skip missions once launched into orbit. This saves much fuel by comparison with landing scenario and launching again for next mission.

Different from Section 4.1.1, the constraints of dynamic pressure are all active in three cases with a value of 13,000 Pa (N/m^2) (see Fig. 7).

Heating flux of third case is significantly higher than the other two because the velocity is much bigger at bottom point in order to go back to 80 km, which can be deduced from Eq. (15).

The load constraint for the first case is the highest and the peak value decreases gradually with decreasing thrust capability.

Thrust capability is the major difference from other re-entry operations. In this part, three scenarios with much smaller thrust capability are presented to show the effect of thrust capability. Furthermore the simulation results demonstrate feasibility of skip SMV with small thrust engine.

4.2. Single objective optimization -to minimize time

In this section, a scenario of minimizing the time is put up because in some emergency circumstances, it is necessary to implement fast skip to retrieve inoperative spacecraft.

Applying similar constraints with Section 4.1.1, the simulation result shows that the minimum time to fulfill skip is about 500 s with only one hop in descent phase. The fuel consumption is quite large which is almost impossible in practice, and more constraints need to be considered (see Fig. 8).

From the subfigure of AoA we can see that the AoA increases to a large value and then falls down quickly. With more strict constraint on control signal, mission time will be prolonged because smaller AoA leads to longer descent time.

In the scenario of minimizing mission time, both constraints of load and dynamic pressure are active. And the peak of heating flux is about 160 $Btu/(ft^2 \cdot s)$ (see Fig. 9).

Although the fuel consumption is quite large and it poses great challenge for the vehicle design, it may play an important role in some emergency situations. For example, if a new launched satellite failed in attitude control or deployed in wrong orbit, it may face collision risk with other space targets, thus it would be necessary to implement prompt retrieval and reduce the risk.

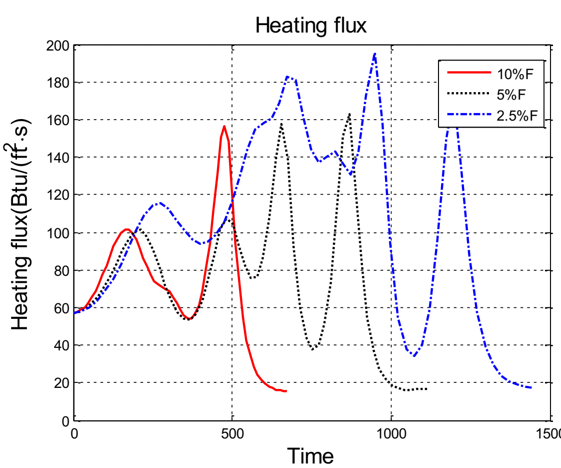

(a) Heating flux time history

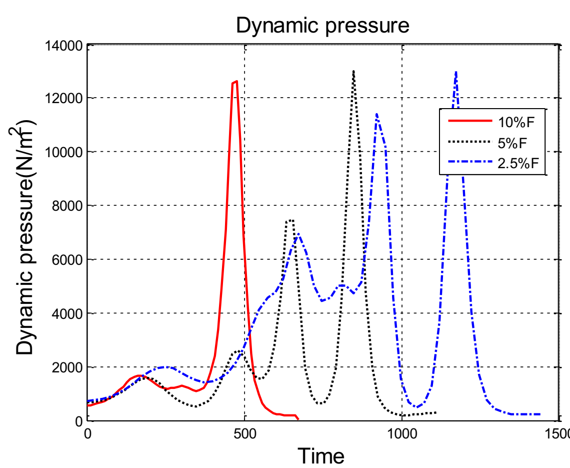

(b) Dynamic pressure time history

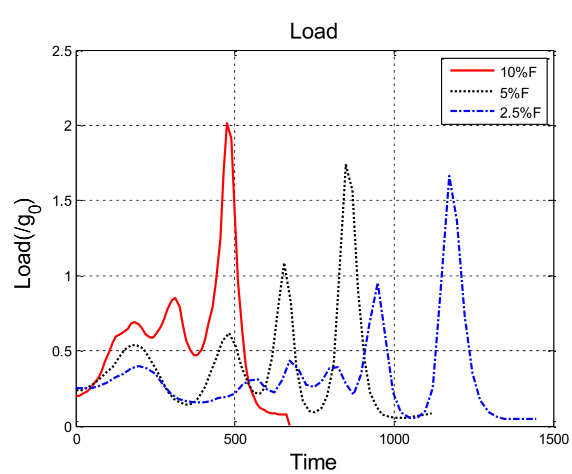

(c) Load time history

Fig. 7. Curves of path constraint.

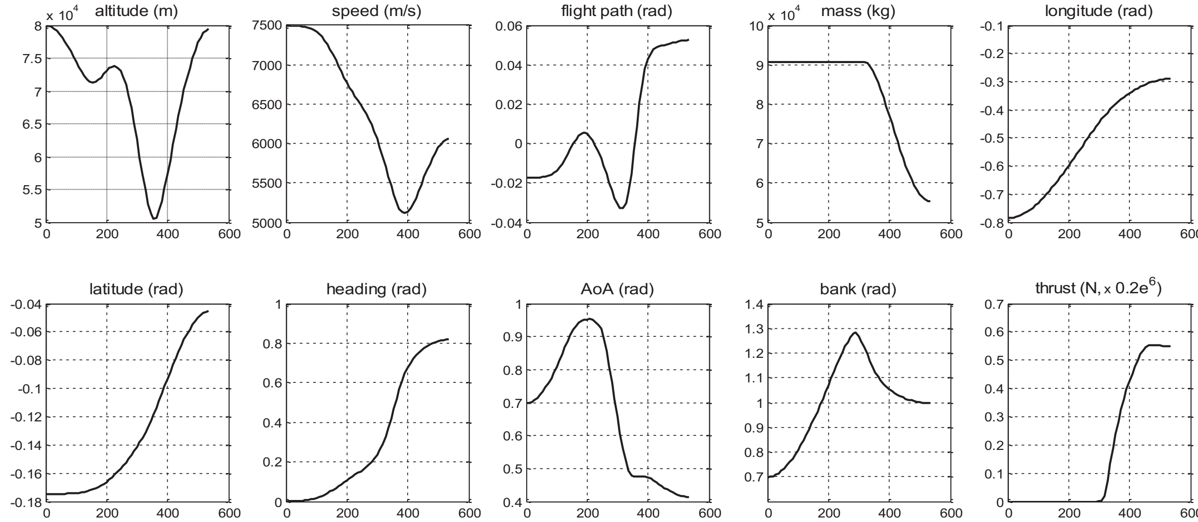

Fig. 8. State curves of minimizing re-entry time.

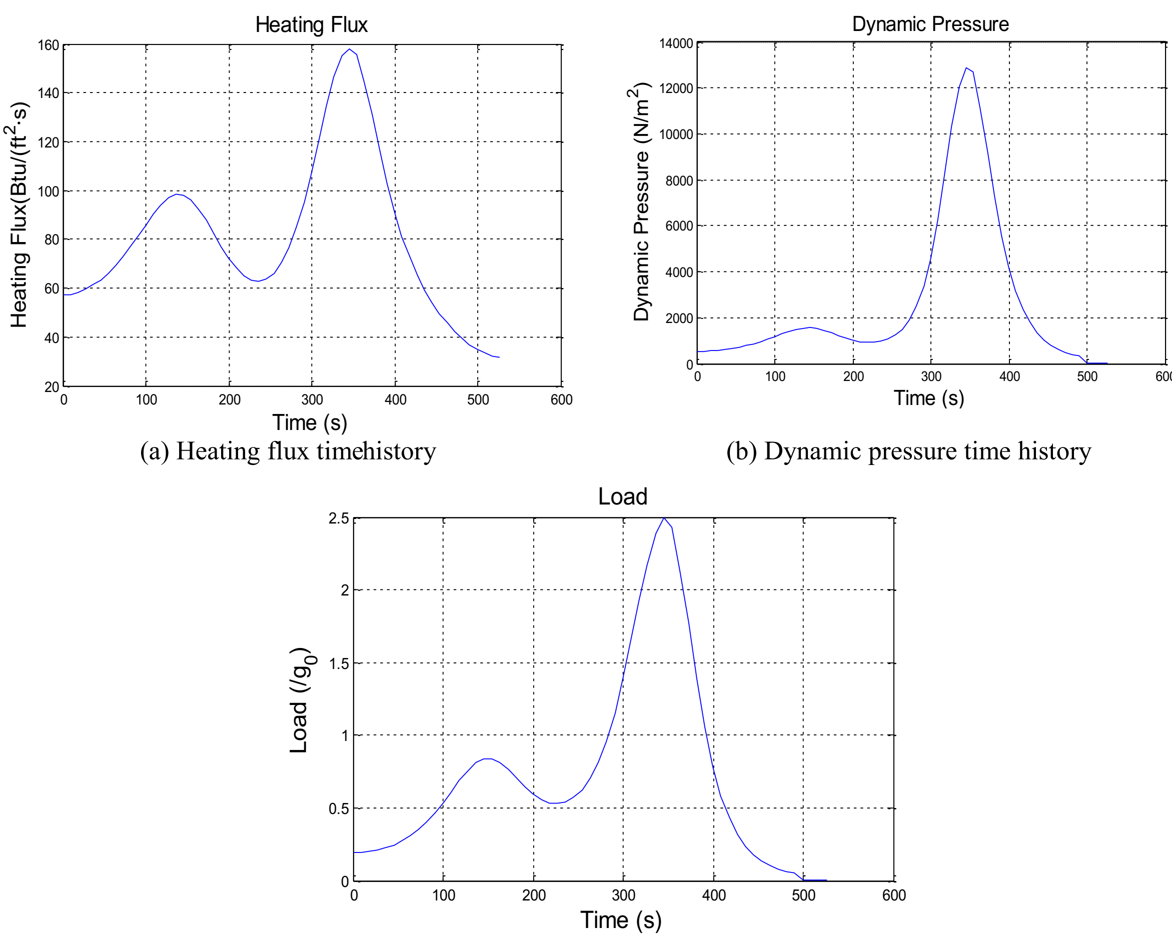

(a) Heating flux timehistory

(b) Dynamic pressure time history

(c) Load time history

Fig. 9. Curves of path constraint.

4.3. Multi objective optimization

In this part, the multi objective optimization simulation is conducted. Three objectives are considered including minimizing time, minimizing fuel consumption and minimizing total heating. In Eq. (14), parameters are set as follows: $J_{imax} = 90{,}719,\ 4000,\ 400{,}000,\ \omega'_i = 0.2,\ 0.4,\ 0.4,\ i = t,\ f,\ h$. Following is simulation results.

Fig. 10 shows the curves of optimized state variables, to be noted, there is one more hop during exit of atmosphere which is quite different from former simulation. Compared with Section 4.1.1, the mission time increases by 50 s and the fuel consumption drops about 2000 kg. The difference in fuel consumption and mission time is minor, however,

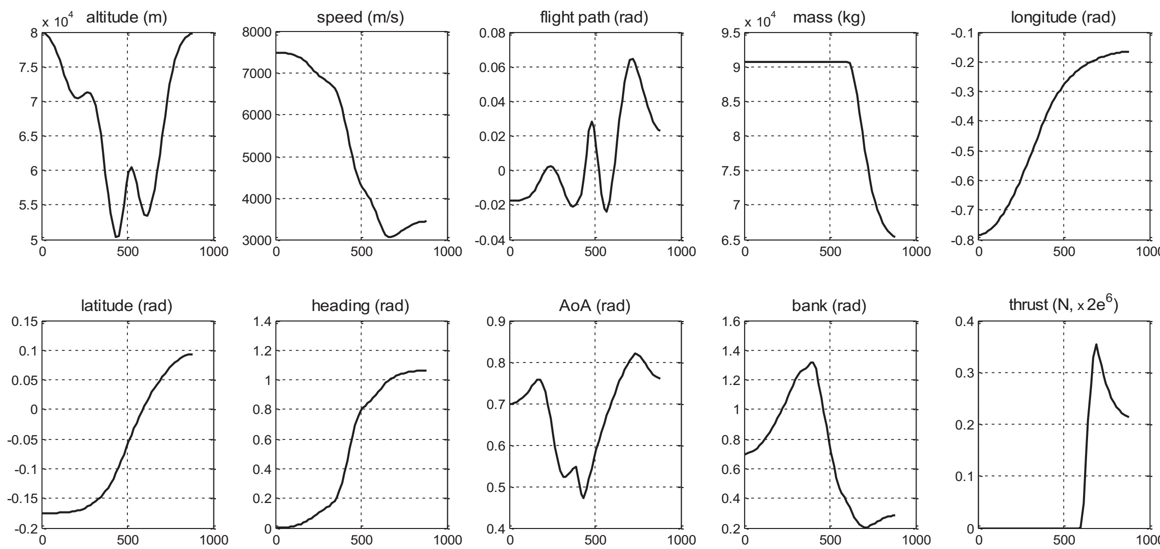

Fig. 10. State curves for multi objective re-entry optimization.

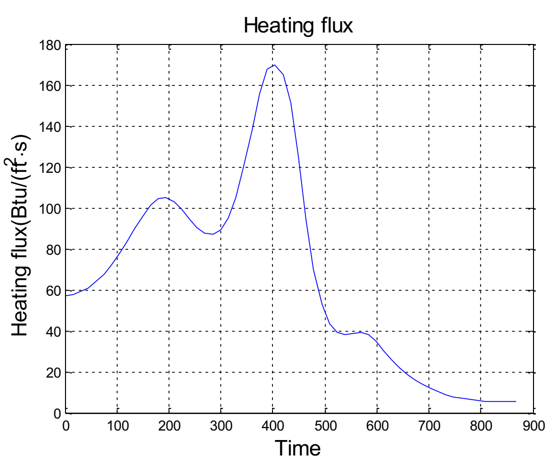

(a) Heating flux time history

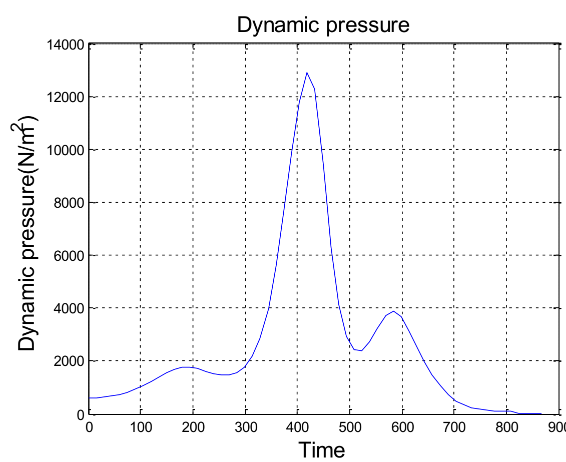

(b) Dynamic pressure time history

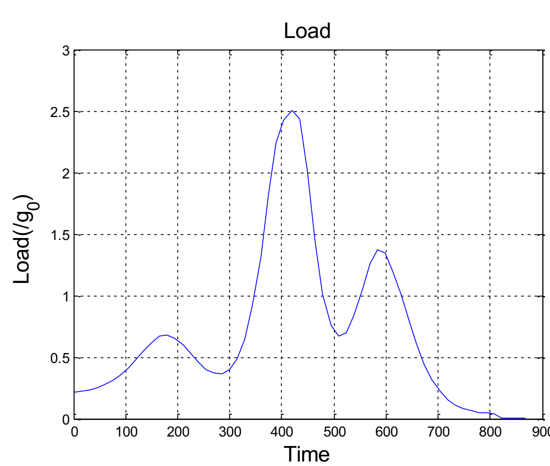

(c) Load time history

Fig. 11. Curves of path constraint.

the difference in total heating is clearly seen from below figures.

Apart from the dynamic pressure, the constraint on load is also active because of larger lift force. From comparison between Figs. 11 and 5, we can see that the total heating is significantly reduced although the maximum value is close. According to above analysis, the total heating plays a remarkable role in optimization objective under current settings of weighting coefficient.

Although the multi objective optimization method achieves a better result in this paper, the performance is affected profoundly by the weighting coefficient of each objective. It is difficult to determine the most appropriate weighting factors. In engineering, decision maker will choose the appropriate value according to experience and prior information. Many scholars have improved multi objective algorithms such as fuzzy satisfactory goal programming method (Hu and Xin, 2015) and design of experiment approach (Bettinger et al., 2015). In the future, more work will be done by applying multi-objective evolution algorithms to skip trajectory optimization to obtain a set of solutions, i.e. Pareto front, rather than just a solution by the weighting method.

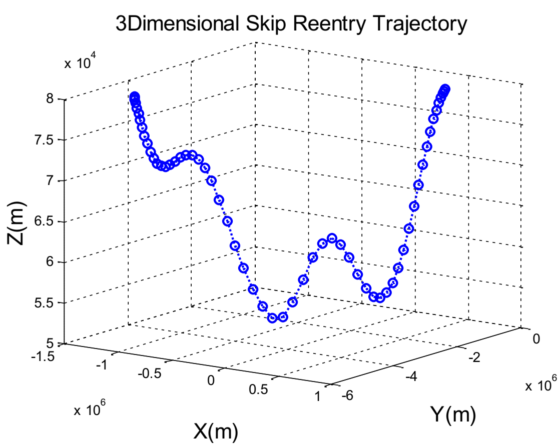

Fig. 12. Three dimensional trajectory of skip SMV.

Fig. 12 shows the three dimensional trajectory of skip SMV, nodes scatter is denser near the boundary based on LGL collocation method.

5. Simulation results of descent to predetermined point

In Section 4, the case of descent to a predetermined altitude is studied. However in some occasions with small re-entry interface window, it is necessary to descend to a position with fixed altitude and longitude to further improve landing precision. In addition, in some cases that have different optimization requirement for descent and exit, it is also necessary to conduct optimization separately in calculating initial value.

In Fig. 13, the line illustrates initial value calculated from GA. The blue line represents optimization result of descent phase, the red line represents exit phase while black circle represents final result by SQP.

From subfigures of longitude and latitude in Figs. 4 and 13, we know that traveled range in the second case is larger than the first one and there are more hops, so we may come to the conclusion that hops can contribute to prolonging the traveled range.

The total number of codes shares the same value with Section 4 which is set as 60, and the number for descent and exit is set to be proportional to the mission time. As the descent phase takes longer time, the number of nodes in descent phase is larger than counterpart in exit phase (see Fig. 14).

Compared with simulation in Section 4, the peak of load and dynamic pressure happens near the bottom point,

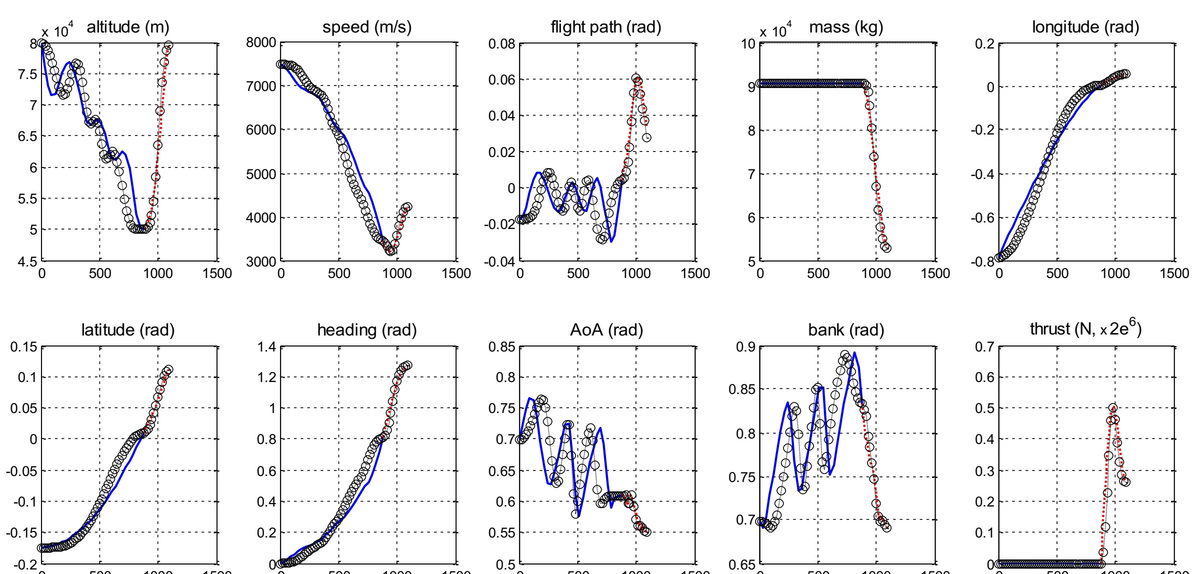

Fig. 13. State curves for re-entry to a predetermined point.

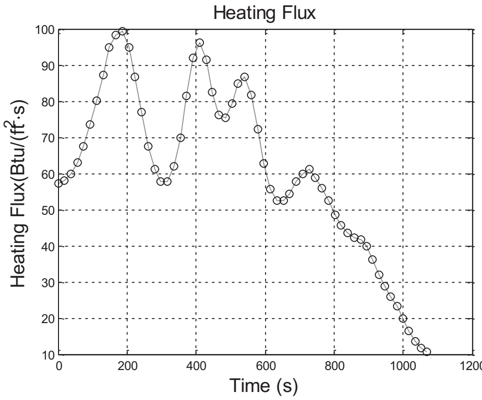

(a) Heating flux time history

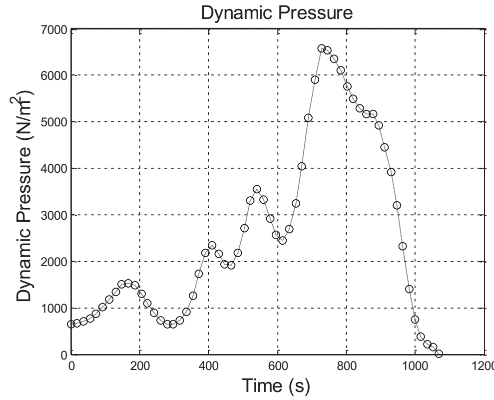

(b) Dynamic pressure time history

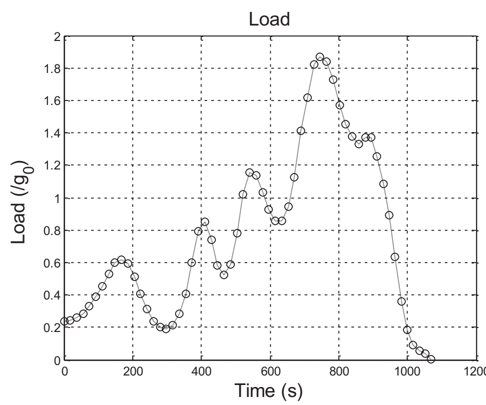

(c) Load time history

Fig. 14. Curves of path constraint.

while the peak of heating flux happens at the initial phase because the total heating is also considered as one optimization objective.

Fig. 15 shows the three dimensional trajectory of skip re-entry with three hops. As the number of nodes is proportional to mission time, the number of nodes in descent phase is much larger than exit phase. Besides, there are more nodes at the bottom point compared with Fig. 12 which performs better for skip re-entry to capture sudden change in state variable.

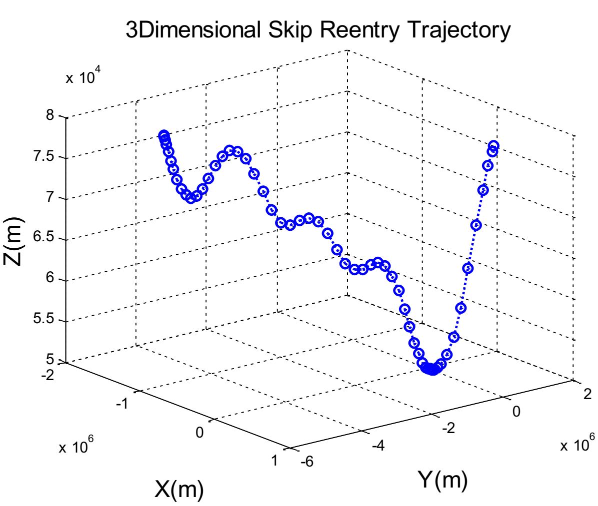

Fig. 15. Three dimensional trajectory of skip SMV.

6. Conclusion

This paper investigates the potential applications of skip SMV and one of the most promising applications is active debris removal. For unusable debris, skip SMV is able to increase the re-entry interface prediction accuracy and reduce risks for people and property on ground. For disabled space property still with value, it is possible for SMV to re-entry to a lower altitude and then release space asset in a cargo, which can help to avoid the breakup brought by atmosphere, and thus improve the landing accuracy.

The key feature of skip trajectory is to descend into atmosphere and then exit. This paper established the dynamic and control equations for skip re-entry with thrust capability. Space shuttle is adopted as the SMV model because the parameter settings are available from open source literatures.

Trajectory optimization is the key issue for skip SMV and it is in detail discussed in our paper with different scenarios. Compared with descent to fixed altitude, descent to predetermined point is more challenging for control. Evolutionary collocation method improves the computation efficiency in skip trajectory optimization. Simulation results demonstrate feasibility of skip SMV in active debris removal satisfying constraints. Although there is no relevant study about the application of skip SMV to removal of large debris, in the future, it will be feasible for skip SMV to perform debris re-entry missions repeatedly and efficiently.

References

Air Force Research Laboratory Space Vehicles Directorate (AFRL/SV), 2004. Space Maneuver Vehicle. http://www.vs.afrl.af.mil/Factsheets/smv.html, 29 January 2004.

Bettinger, R.A., Black, J.T., 2014. Comparative study of phasing, atmospheric skip entry, and simple plane change maneuvers. J. Spacecraft Rockets 51 (6), 1965–1975.

Bettinger, R.A., Black, J.T., Agte, J.S., 2015. Design of experiment approach to atmospheric skip entry maneuver optimization. J. Spacecraft Rockets 52 (3), 813–826.

Betts, J.T., 1998. Survey of numerical methods for trajectory optimization. J. Guid. Control Dyn. 21 (2), 193–207.

Betts, J.T., 2010. Practical Methods for Optimal Control and Estimation using Nonlinear Programming, vol. 19. SIAM.

Bonnal, C., Ruault, J.M., Desjean, M.C., 2013. Active debris removal: recent progress and current trends. Acta Astronaut. 85, 51–60.

Bottacini, M., Berthe, P., Vo, X., et al., 2011. The advanced re-entry vehicle (ARV) a development step from ATV toward manned transportation systems. ESA Special Publication 692, 118.

Du, X., Li, H.Y., Shen, H.X., 2014. Skip reentry trajectory optimization based on analysis of path constraints. Acta Aeronaut. Astronaut. Sin. 35 (5), 1265–1275.

Duan, H.B., Li, S., 2015. Artificial bee colony based direct collocation for reentry trajectory optimization of hypersonic vehicle. IEEE Trans. Aerosp. Electron. Syst. 51 (1), 615–626.

Fahroo, F., Ross, I.M., 2008. Advances in pseudospectral methods for optimal control. In: AIAA Guidance, Navigation and Control Conference and Exhibit.

Gill, P.E., Wong, E., 2012. Sequential quadratic programming methods. In: Mixed Integer Nonlinear Programming. Springer, New York, pp. 147–224.

Grantz, A.C., 2011. X-37B orbital test vehicle and derivatives. In: AIAA SPACE 2011 Conference & Exposition. AIAA-2011-7315.

Howard, R.D., Krevor, Z.C., Mosher, T., et al., 2011. Dream chaser commercial crewed spacecraft overview. In: 17th AIAA International Space Planes and Hypersonic Systems and Technologies Conference.

Hu, C.F., Xin, Y., 2015. Reentry trajectory optimization for hypersonic vehicles using fuzzy satisfactory goal programming method. Int. J. Autom. Comput. 12 (2), 171–181.

Kai, U.S., Peter, L.H., Jana, R., et al., 2015. Handbook of Space Security: Policies, Applications and Programs, 2015th ed. Springer, New York.

Liou, J.C., 2011. An active debris removal parametric study for LEO environment remediation. Adv. Space Res. 47 (11), 1865–1876.

Moshman, N.D., Proulx, R.J., 2014. Range improvements in gliding reentry vehicles from thrust capability. J. Spacecraft Rockets 51 (5), 1681–1694.

Properties of a standard atmosphere, ESDU Item No. 77021, Royal Aeronautical Society, 1 March, 2005.

Virgili, J., Roberts, P.C.E., Hara, N.C., 2015. Atmospheric interface reentry point targeting using aerodynamic drag control. J. Guid. Control Dyn. 38, 1–11.

Wang, W.L., Leonard, J., Savvaris, A., Tsourdos, A., 2015. Evolutionary collocation methods for SMV skip trajectory optimization. In: 6th European Conference for Aeronautics and Space Sciences, Poland.

Zhao, J., Zhou, R., Jin, X., 2014. Progress in reentry trajectory planning for hypersonic vehicle. J. Syst. Eng. Electron. 25 (4), 627–639.

Zondervan, K., 1984. Solving the optimal control problem using a nonlinear programming technique, Part 3: Optimal shuttle reentry trajectories. In: Proceedings of the AIAA/AAS Astrodynamics Conference, AIAA-84-2039, Seattle, WA.